

**Fermi National Accelerator Laboratory**

**FERMILAB Conf-96/299-E  
DØ**

**Measurement of  $\sigma (p\bar{p} \rightarrow t\bar{t})$  at  $\sqrt{s} = 1.8$  TeV  
by the DØ Experiment**

**John M. Butler**  
*Boston University*  
*590 Commonwealth Avenue, Boston MA 02215*

**Dhiman Chakraborty**  
*Department of Physics*  
*State University of New York, Stony Brook*  
*New York 11794*

**For the DØ Collaboration**  
*Fermi National Accelerator Laboratory*  
*P.O. Box 500, Batavia, Illinois 60510-0500*

**September 1996**

Published Proceedings of the *XI Topical Workshop on  $\bar{p}p$  Collider Physics*, Abano Terme (Padova), Italy,  
May 27-June 1, 1996.

## **Disclaimer**

*This report was prepared as an account of work sponsored by an agency of the United States Government. Neither the United States Government nor any agency thereof, nor any of their employees, makes any warranty, express or implied, or assumes any legal liability or responsibility for the accuracy, completeness or usefulness of any information, apparatus, product or process disclosed, or represents that its use would not infringe privately owned rights. Reference herein to any specific commercial product, process or service by trade name, trademark, manufacturer or otherwise, does not necessarily constitute or imply its endorsement, recommendation or favoring by the United States Government or any agency thereof. The views and opinions of authors expressed herein do not necessarily state or reflect those of the United States Government or any agency thereof.*

## **Distribution**

*Approved for public release: further dissemination unlimited.*

# Measurement of $\sigma(p\bar{p} \rightarrow t\bar{t})$ at $\sqrt{s} = 1.8$ TeV by the DØ Experiment

John M. Butler

*Boston University*

*590 Commonwealth Avenue, Boston MA 02215, USA*

Dhiman Chakraborty

*Department of Physics,*

*State University of New York, Stony Brook,*

*NY 11794, USA*

(for the DØ Collaboration)

We present the results from counting  $t\bar{t}$  event candidates in  $p\bar{p}$  collisions at a center-of-mass energy of 1.8 TeV by the DØ collaboration. The results are based on an analysis of  $\sim 100$  pb $^{-1}$  of data in seven different channels which can be broadly categorized as dilepton or single-lepton depending on whether there are two or one high- $p_T$  isolated leptons ( $e$  or  $\mu$ ) in the final state. We have three dilepton channels,  $ee$ ,  $\mu\mu$  and  $e\mu$ . The single-lepton analysis is further divided into two subcategories, event shape and tag, orthogonal by construction, each of which has two channels,  $e + jets$  and  $\mu + jets$ . All channels combined, we observe 37 events in our data with an estimated background of  $13.4 \pm 3.0$  events. Under the assumptions of the minimal standard model, this translates into a  $t\bar{t}$  production cross section as a function of the mass of the top quark ( $m_t$ ). For  $m_t = 180$  GeV, our measurement amounts to  $\sigma(p\bar{p} \rightarrow t\bar{t}) = 4.7 \pm 1.6$  pb.

## 1 Introduction

The long search for the top quark ended a little over a year ago with the simultaneous announcement of the top quark discovery by the DØ and CDF collaborations<sup>1,2</sup>. The DØ results were based on an integrated luminosity of approximately 50 pb $^{-1}$  where 17 candidate events were observed with an estimated background of  $3.8 \pm 0.6$  events. The top mass was measured to be  $199_{-21}^{+19}(\text{stat.})_{-21}^{+14}(\text{syst.})$  GeV and the top pair production cross section to be  $6.2 \pm 2.2$  pb. Since the initial observation, significant progress has been made in the DØ top quark analysis. The report on the preliminary results from the updated analysis presented here is organized as follows: after a brief introduction to top physics at the Tevatron, improvements in the analysis are outlined, the details of the study of the top quark in single-lepton and dilepton final states and finally the measurement of the cross section are given. All along, we confine ourselves to the premises of the minimal Standard Model.

### 1.1 Top Quark Production and Decay

At the Tevatron center-of-mass energy of  $\sqrt{s} = 1.8$  TeV, top pair production dominates the production of single top by about a factor of 2–3, depending on  $m_t$ . Of the pair-produced top quarks,  $\sim 90\%$  result from  $q\bar{q} \rightarrow t\bar{t}$  and the rest from  $gg \rightarrow t\bar{t}$ <sup>3</sup>. Our selection criteria are optimized for the detection of top quarks produced in pairs.

In the minimal Standard Model a top quark decays exclusively through the weak charged current *i.e.*  $\text{BR}(t \rightarrow Wb) = 1$ . The decay modes of the  $t\bar{t}$  system are classified according to the decay modes of the two  $W$ 's. The “dilepton” modes  $t\bar{t} \rightarrow ee + jets$ ,  $\mu\mu + jets$  ( $\text{BR} = 1/81$  each),  $t\bar{t} \rightarrow e\mu + jets$  ( $\text{BR} = 2/81$ ) and the “lepton +jets” modes  $t\bar{t} \rightarrow e + jets$ ,  $\mu + jets$  ( $\text{BR} = 12/81$  each) are covered here. Analyses of the modes where at least one  $W$  decays into a  $\tau$  lepton ( $\text{BR} = 17/81$ ) are made difficult by the challenging task of identification of  $\tau$  leptons in the  $p\bar{p}$  collider environment and are still in progress. Results from the “all jets” mode where both the  $W$ 's decay into quarks ( $\text{BR} = 36/81$ ) can be found in Ref.<sup>4</sup>.

### 1.2 Modeling of the Signal and the Backgrounds

For the simulation of signal, we have used the ISAJET<sup>5</sup> event generator to produce events for several values of  $m_t$  between 120 GeV and 220 GeV. No restriction was applied to the decay products of the top. GEANT<sup>6</sup> was used to model the detector response. For physics backgrounds, PYTHIA<sup>7</sup> was used for the dilepton analyses. For the single-lepton analyses, VECBOS<sup>8</sup> was used to model the kinematics of the chief physics background,  $W + jets$ , but the overall normalization was derived from the  $D\bar{O}$  data sample itself (see section 3 for details). The Monte Carlo events were subject to the same selection criteria as the data, including a simulation for the triggers. The systematic uncertainties include variation of the jet energy scale by one standard deviation, differences between HERWIG<sup>9</sup> and ISAJET Monte Carlo programs as well as uncertainties in lepton identification and momentum measurements, trigger efficiencies and luminosity.

### 1.3 Improvements Since Observation

There have been a number of significant improvements in the  $D\bar{O}$  top quark analysis since the discovery of top. The first such is statistical: the data set represented here is approximately  $100 \text{ pb}^{-1}$  which is  $\sim 90\%$  of the entire Tevatron Run 1. This is twice the integrated luminosity on which the discovery was based. The next area of improvement is in new, more powerful particle

identification. Employing a four-variable likelihood technique, the electron-identification retains its former efficiency while achieving a 20–30% reduction in fake electron background. Similarly, the new muon identification has  $\sim 10\%$  better efficiency while lowering the background, for example, by a factor of 2–3 for non-isolated muons. In addition, there were two substantial gains in top acceptance for final states containing muons. The first was from a new  $\mu + jets$  trigger that raised the trigger efficiency in this mode from 70% to 95%. The second was extending the geometric acceptance for muons from  $\eta_{max} = 1.0$  to  $\eta_{max} = 1.7$  by solving a problem of aging in the forward muon chambers. Also, an improved understanding of the jet energy scale has contributed to the reduction of the systematic uncertainties. Finally, the precision of this analysis has benefited from a new optimization of selection criteria which will be discussed below.

## 2 Top Pair Decay in the Dilepton Channels

The dilepton channels,  $t\bar{t} \rightarrow W(\rightarrow \ell_1\nu)W(\rightarrow \ell_2\nu)b\bar{b}$  where  $\ell_{1,2} = e$  or  $\mu$ , have the following general characteristics:

- two high- $p_T$  isolated leptons (from the leptonic decay of two  $W$ 's),
- large missing transverse energy ( $\cancel{E}_T$ ) carried away by two neutrinos (also from the leptonic decay of two  $W$ 's),
- at least two jets (one from each  $b$ ).

The distributions of lepton  $p_T$ ,  $\cancel{E}_T$  and the number of jets with  $E_T > 20$  GeV,  $\eta < 2.5$  for the signal, the major backgrounds and our data in the  $e\mu$  channel are shown in Fig. 1(a), Fig. 1(b) and Fig. 1(c) respectively. Finally, we construct a variable called  $H_T$  which is the scalar sum of of the  $E_T$ 's of all the jets and the highest- $E_T$  electron in an event. Muons are excluded from this construction due to their poorer momentum resolution. The distributions of  $H_T$  for  $e\mu$  events from expected signal and the combined backgrounds are shown in Fig. 1(d). The complete set of selection cuts for the different channels are listed in Table 1.

The background contributions to our candidate sample are listed in Table 2. The dominant source of background varies from channel to channel. The requisite amount of  $\cancel{E}_T$  can arise in background events either from real neutrinos or from mismeasurement of the momenta of other particles in the event. Hence, for  $ee$ , the largest contribution comes from occasional misidentification of hadron-initiated showers as electrons. Although  $Z(\rightarrow ee) + jets$  is a major source of two high- $p_T$  electrons plus jets, this background can be effectively

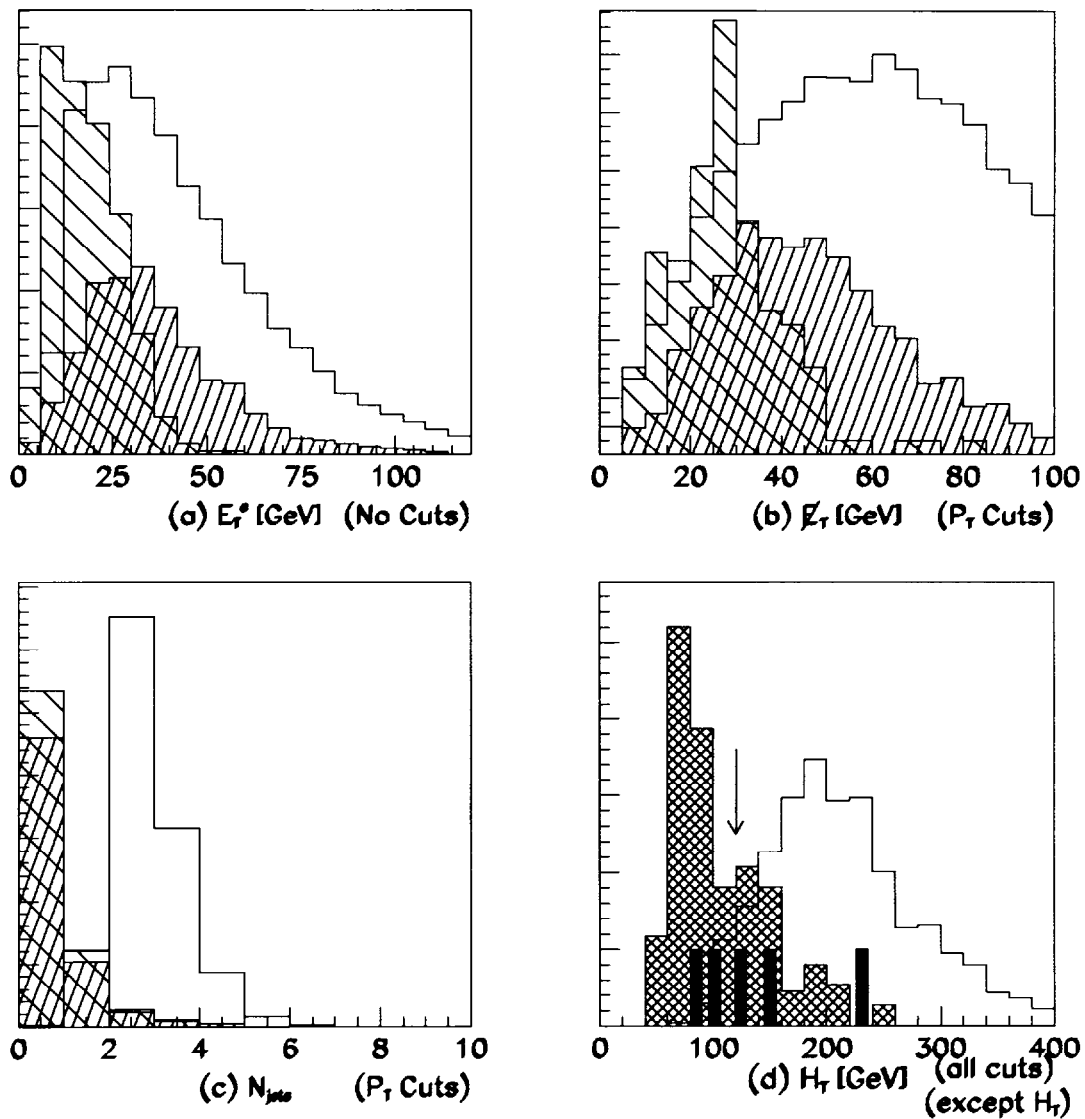


Figure 1: Distribution of selection variables for signal and backgrounds in the  $e\mu$  channel. In (a)-(c), the lightly and heavily hatched histograms represent the  $Z \rightarrow \tau\tau$  and  $WW$  backgrounds respectively while the blank histograms represent the expected signal behavior. In (d), the hatched histogram represents the combined background, the blank histogram represents the simulated signal and the solid entries represent the  $D0$  events passing all the previous cuts. The arrow indicates the cut (minimum requirement).

Table 1: Selection criteria for the various dilepton channels.

Object	Selection cuts in different channels		
	$ee$	$\mu\mu$	$e\mu$
$p_T(\ell)$	$> 15$ GeV	$> 20$ GeV	$> 15$ GeV
$ \eta(e) $	$< 2.5$	–	$< 2.5$
$ \eta(\mu) $		$< 1.0$	$< 1.7$
$\cancel{E}_T$	$> 25$ GeV	–	$> 20$ GeV
$E_T(j)$	$> 20$ GeV	$> 20$ GeV	$> 20$ GeV
$ \eta(j) $	$< 2.5$	$< 2.5$	$< 2.5$
$n(j)$	$\geq 2$	$\geq 2$	$\geq 2$
$m_{\ell\ell}$ etc	$\cancel{E}_T > 40$ GeV if $ m_{ee} - m_Z  < 12$ GeV	$Z$ -fitter, $m_{\mu\mu} > 10$ GeV, $ \Delta\eta(\mu, \mu)  < 0.5$ if $ \Delta\phi(\mu, \mu)  > 160^\circ$	–
$H_T$	$> 120$ GeV	$> 120$ GeV	$> 100$ GeV

suppressed, without sacrificing too much of our signal, by requiring the  $\cancel{E}_T$  to be higher if the invariant mass of the two electrons is too close to  $m_Z$ .  $Z(\rightarrow \tau\tau) + jets$  with both  $\tau$ 's decaying into electrons is harder to suppress because  $m_Z - m_{ee}$  is usually not small and there are real neutrinos in the event to give a substantial  $\cancel{E}_T$ . Other backgrounds turn out to be negligible compared to these three. For  $\mu\mu$ , the scenario is similar in principle, but because of the poor resolution of the muon momentum at such high values, instead of placing separate cuts on  $\cancel{E}_T$ ,  $m_{\mu\mu}$  etc, events are subjected to a fitting procedure trained on  $Z(\rightarrow \mu\mu) + jets$  events and those with a high probability of having come from this source are rejected. Still,  $Z(\rightarrow \mu\mu) + jets$  accounts for nearly 85% of the total background in this channel. The rest is due to muons from semi-leptonic decays of high- $p_T$  heavy quarks ( $b, c$ ) that move away far enough from the rest of the jet to look like isolated muons from  $W \rightarrow \mu\nu$ . Contributions from lower resonances (e. g.  $J/\psi$ ) and cosmic muons are reduced to negligible levels by cuts on the invariant mass and the angle between the two muons respectively. Being free from the background of Drell-Yan production of  $ee$  or  $\mu\mu$ ,  $e\mu$  is the cleanest of the three dilepton channels.  $Z(\rightarrow \tau\tau) + jets$  with one tau decaying into an electron and the other into a muon accounts for 85% of the total background. The rest comes from  $WW(\rightarrow e\mu\nu_e\nu_\mu) + jets$ ,  $Z^*/\gamma^*(\rightarrow \tau\tau) + jets$  and fake electrons.

The results of the dilepton analysis are summarized in Table 2. We observe 5 events in our data sample with an expected contribution of  $1.57 \pm 0.34$  events from background processes. We also note that the total expected signal for  $m_t = 180$  GeV is  $3.14 \pm 0.31$  events.

Table 2: Expected top yields, estimated backgrounds and the number of events in  $D\bar{O}$  data satisfying the dilepton selection criteria.

		$ee$	$\mu\mu$	$e\mu$
$\int \mathcal{L} dt$		$105.9 \text{ pb}^{-1}$	$86.7 \text{ pb}^{-1}$	$90.5 \text{ pb}^{-1}$
Top yield	$m_t = 150 \text{ GeV}$	$1.99 \pm 0.25$	$0.92 \pm 0.19$	$3.40 \pm 0.55$
	$m_t = 180 \text{ GeV}$	$0.92 \pm 0.11$	$0.53 \pm 0.11$	$1.69 \pm 0.27$
	$m_t = 200 \text{ GeV}$	$0.59 \pm 0.07$	$0.27 \pm 0.06$	$1.00 \pm 0.16$
	$m_t = 220 \text{ GeV}$	$0.31 \pm 0.04$	$0.15 \pm 0.03$	$0.55 \pm 0.09$
Back- grounds	$Z \rightarrow ee / Z \rightarrow \mu\mu$	$0.13 \pm 0.03$	$0.464 \pm 0.261$	-
	$Z \rightarrow \tau\tau$	$0.17 \pm 0.04$	$0.028 \pm 0.008$	$0.305 \pm 0.070$
	$WW$	$0.04 \pm 0.02$	$0.009 \pm 0.003$	$0.027 \pm 0.012$
	fake $e / \mu$ from $b, c$	$0.32 \pm 0.14$	$0.047 \pm 0.010$	$0.016 \pm 0.004$
Total background		$0.66 \pm 0.17$	$0.55 \pm 0.28$	$0.36 \pm 0.09$
Data		1	1	3

### 3 Top Pair Decay in the Lepton + Jets Channels

The lepton + jets mode,  $t\bar{t} \rightarrow W(\rightarrow \ell\nu)W(\rightarrow q\bar{q}')b\bar{b}$ , has the following general characteristics: one high- $p_T$  isolated lepton ( $\ell = e$  or  $\mu$ ), large  $\cancel{E}_T$  (both resulting from the leptonic  $W$  decay) and high jet multiplicity (nominally four jets: two from the  $b$  quarks and two from the hadronic  $W$  decay).

We divide the principal backgrounds to the lepton + jets mode into two categories: physics and instrumental. Physics backgrounds arise from other physics processes which mimic the lepton + jets topology. By far, the dominant physics background is  $p\bar{p} \rightarrow W(\rightarrow \ell\nu) + jets$ . The next largest,  $Z(\rightarrow \ell\ell) + jets$ , is an order of magnitude smaller than  $W + jets$ . Instrumental backgrounds arise from multi-jet events where the lepton is a “fake”: either a jet is misidentified as an electron or a muon in a jet is misidentified as an isolated muon. Other sources of background are found to be negligible.

The lepton + jets analysis begins by selecting events with a high- $p_T$  isolated lepton, large  $\cancel{E}_T$ , and at least one jet. Figure 2 shows the number of  $W + jets$  events from Run 1  $D\bar{O}$  data as a function of the minimum number of jets observed in the event. Also plotted are the number of events expected from top with  $m_t = 180 \text{ GeV}$ . From Fig. 2 it is clear, even at the nominal lepton + jets multiplicity of four, that the data is dominated by  $W + jets$  background and additional background rejection is necessary to extract the top signal. We get the additional rejection through two strategies: the first method makes

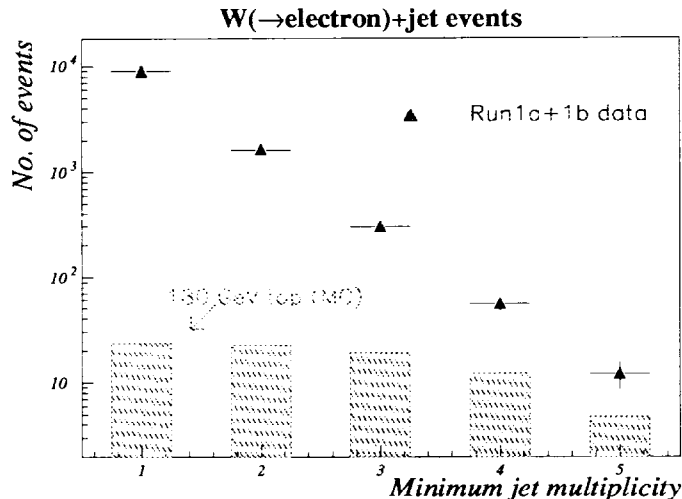


Figure 2: The number of  $W(\rightarrow e\nu) + jets$  events as a function of the minimum jet multiplicity. Also shown is the expectation for 180 GeV top events.

hard cuts on event shape variables to distinguish top from background and the second method requires at least one of the  $b$  quarks from top decay to be tagged by a non-isolated muon. The two analyses are made orthogonal by construction so that the results can be combined simply.

### 3.1 Event Shape Analysis

The event shape analysis begins by selecting events with a high- $p_T$  electron or muon, large  $\cancel{E}_T$ , and at least 4 jets. Events with a tag muon, as described in the tag analysis later, are vetoed. Cuts on three event shape variables are then applied:

- Total leptonic  $E_T$ :  $E_T^L \equiv E_T(\ell) + \cancel{E}_T$ . A cut requiring large  $E_T^L$  is effective at rejecting multi-jet background.
- Hadronic activity:  $H_T \equiv \sum E_T(j)$ . Lepton + jets events nominally have four high energy jets which, because top is so massive, tend to be central. Therefore top events will generally have higher  $H_T$  than the backgrounds.
- Aplanarity:  $\mathcal{A} \equiv 3/2$  times the smallest eigenvalue of the normalized momentum tensor constructed from the  $W$  and jets. Defined in this way,

$\mathcal{A} = 0.5$  for spherical events and  $\mathcal{A} = 0$  for planar or linear events. Aplanarity exploits the fact that top events tend to be rather spherical while the radiative backgrounds tend to be more planar.

The exact values of the cuts are listed in Table 3. The cut boundaries were chosen using a new optimization procedure which represents a change in focus for the analysis. When searching for top, the cuts were optimized for signal significance. Now that the existence of top has been established, we want to measure top quark properties. In this analysis, the goal of the new optimization is to minimize the error on the top production cross section and that condition determines the values in Table 3.

The instrumental background is calculated from the data. The probability for a misidentified isolated lepton  $P_{\ell}$  is determined from low  $\cancel{E}_T$  data which is dominated by fakes.  $P_{\ell}$  is then convoluted with multi-jet data to give the number of background events.

The  $W + jets$  background is calculated under the assumption that the number of background events falls off exponentially with increasing jet multiplicity (“Berends scaling”) <sup>10</sup>. A variety of data sets ( $Z + jets$ ,  $\gamma + jets$ , multi-jets) have been shown to follow this scaling very well <sup>11</sup>. The idea here is to use the low jet multiplicity  $W + jets$  data, which has very little top, to predict the  $W + jets$  background for events with  $\geq 4$  jets. Berends scaling only predicts the shape of the multiplicity distribution, the normalization comes from the data. Thus this procedure avoids using a Monte Carlo prediction for the background normalization. Figure 3 shows the jet multiplicity distribution for the  $\mu + jets$  channel before the shape cuts are applied. For the lower jet threshold, where background is more prevalent, the Berends scaling behavior is evident. At the higher jet threshold, the top signal begins to emerge for  $\mu + \geq 4$  jets.

The results of the event shape analysis are summarized in Table 4. From  $\approx 106 \text{ pb}^{-1}$  of integrated luminosity, we observe 21 events passing the event shape analysis cuts, 10 in the  $e + jets$  channel and 11 in the  $\mu + jets$  channel, with an estimated background of  $9.2 \pm 2.8$  events. The expected top yields in Table 4 were calculated using the central value cross section of Ref. <sup>3</sup>. For  $m_t = 180 \text{ GeV}$ , we would expect about 12.9 top events in the sample.

### 3.2 Tag Analysis

The tag analysis exploits the fact that the main source of background,  $W + jets$ , has relatively little heavy flavor content compared to top. The tagging of heavy flavor jets thus provides a good handle for rejecting background. Top events are rich in heavy flavor by virtue of the 2  $b$  quarks and  $\sim 2.5$   $c$  quarks per event. About 40% of all top events have a muon from the semileptonic decays

Table 3: Selection criteria for the various lepton + jets channels.

Channel	Event Shape Analysis		Tag Analysis	
	$e + jets$	$\mu + jets$	$e + jets + tag$	$\mu + jets + tag$
Lepton	$E_T(e) > 20 \text{ GeV}$ $ \eta(e)  < 2$	$p_T(\mu) > 20 \text{ GeV}$ $ \eta(\mu)  < 1.7$	$E_T(e) > 20 \text{ GeV}$ $ \eta(e)  < 2$	$p_T(\mu) > 20 \text{ GeV}$ $ \eta(\mu)  < 1.7$
Neutrino	$\cancel{E}_T > 25 \text{ GeV}$	$\cancel{E}_T > 20 \text{ GeV}$	$\cancel{E}_T > 20 \text{ GeV}$	$\cancel{E}_T > 20 \text{ GeV}$
Jets	$\geq 4$ jets with $E_T > 15 \text{ GeV}$ and $ \eta  < 2$		$\geq 3$ jets with $E_T > 20 \text{ GeV}$ and $ \eta  < 2$	
Shape Cuts	$E_T^L > 60 \text{ GeV}$ $\mathcal{A} > 0.065$ $H_T > 180 \text{ GeV}$		— $\mathcal{A} > 0.04$ $H_T > 110 \text{ GeV}$	
Soft muon tag	Vetoed		$p_T > 4 \text{ GeV}$ and $\Delta R < 0.5$	

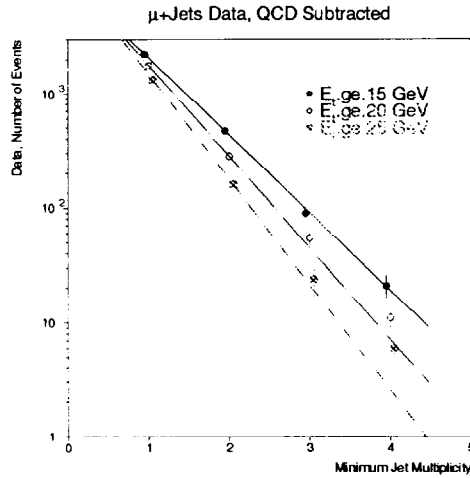


Figure 3: The number of  $\mu + jets$  events as a function of minimum jet multiplicity for three values of the minimum jet  $E_T$ . The event shape cuts have not been applied.

Table 4: Expected top yields, estimated backgrounds, and data satisfying the lepton + jets selection criteria.

Top Yields	$\ell + jets$	$\ell + jets + tag$
$m_t = 140$ GeV	$31.9 \pm 5.9$	$12.5 \pm 2.7$
$m_t = 160$ GeV	$18.8 \pm 3.3$	$9.0 \pm 2.2$
$m_t = 180$ GeV	$12.9 \pm 2.3$	$5.2 \pm 1.3$
$m_t = 200$ GeV	$7.7 \pm 1.4$	$3.4 \pm 0.9$
Background	$\ell + jets$	$\ell + jets + tag$
$W + jets$	$7.68 \pm 2.77$	$1.84 \pm 0.39$
QCD (fake lepton)	$1.55 \pm 0.49$	$0.62 \pm 0.20$
$Z \rightarrow \mu\mu$	-	$0.12 \pm 0.06$
Total	$9.23 \pm 2.83$	$2.58 \pm 0.57$
Data	$10 e + jets$	$5 \ell + jets + tag$
	$11 \mu + jets$	$6 \mu + jets + tag$

$b, c \rightarrow \mu$ . The efficiency for one of these muons to pass the tag  $\mu$  selection is  $\approx 50\%$ . Therefore  $\approx 20\%$  of all top events will have an identified tag  $\mu$  compared to  $\approx 2\%$  of  $W + \geq 3 jets$  events.

While the  $b, c \rightarrow \mu$  branching ratio and tag  $\mu$  efficiency does reduce the overall top acceptance, the improved signal-to-noise from the tag allows us to relax other cuts to regain efficiency. The event selection begins as before by requiring a high- $p_T$  isolated lepton, large  $\cancel{E}_T$ , and  $\geq 3$  jets. A tag muon is required which has  $p_T > 4$  GeV and must be non-isolated, where non-isolated is defined as the muon being within  $\Delta R = 0.5$  in  $\eta - \phi$  space of a jet. Finally, a set of event shape cuts are applied. The values of the cuts are listed in Table 3 where it is seen that the cuts are generally looser: the minimum number of jets have gone down from four to three (albeit the minimum requirement on the  $E_T$  is increased from 15 GeV to 20 GeV), the  $H_T$  and  $\mathcal{A}$  cuts are relaxed, and the  $E_T^L$  cut has been dropped.

The multi-jet background is calculated from the data just as in the event shape analysis. Unlike the event shape analysis, the  $W + jets$  background in the tag analysis is derived directly from the data. The background calculation starts with the sample before tagging. After correcting for the small multi-jet component, the data are essentially all  $W + jets$  events. We then convolute the jet multiplicity spectrum of the untagged sample with the tag-rate/jet to determine the number of  $W + jets$  background events. The tag rate is roughly 0.4%/jet and is determined from multi-jet data.

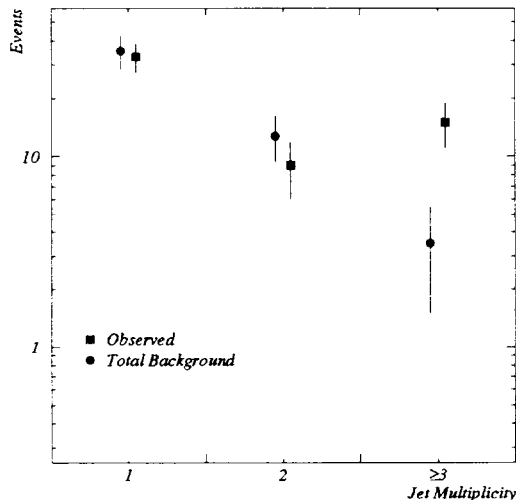


Figure 4: The number of  $\ell + jets + tag$  events (circles) and the total estimated background (squares) as a function of jet multiplicity. The event shape cuts have not been applied.

Figure 4 shows the jet multiplicity distribution for the combined  $e + jets + tag$  and  $\mu + jets + tag$  channels before the shape cuts are applied. Also shown is the total estimated background which agrees very well with the data at low jet multiplicity where there is little top contribution. The excess of events at high jet multiplicity is indicative of the emerging top signal.

The results of the tag analysis are summarized in Table 4. From  $\approx 96 \text{ pb}^{-1}$  of integrated luminosity, we observe 11 events passing the tag analysis cuts, 5 in the  $e + jets + tag$  channel and 6 in the  $\mu + jets + tag$  channel, with an estimated background of  $2.6 \pm 0.6$  events. The expected top yields are also shown in Table 4; for  $m_t = 180 \text{ GeV}$ , we would expect about 5.2 top events in the sample.

#### 4 Top Pair Production Cross section at the Tevatron

Each of the analyses of the dilepton and single-lepton channels described in the preceding sections lead to a calculation of the cross section for the process  $p\bar{p} \rightarrow t\bar{t}$  at  $\sqrt{s} = 1.8 \text{ TeV}$  for a given  $m_t$ . These agree very well with each other within uncertainties (see Table 5). Finally, we combine all these channels to calculate a single cross section. For  $m_t = 180 \text{ GeV}$ , our calculation yields

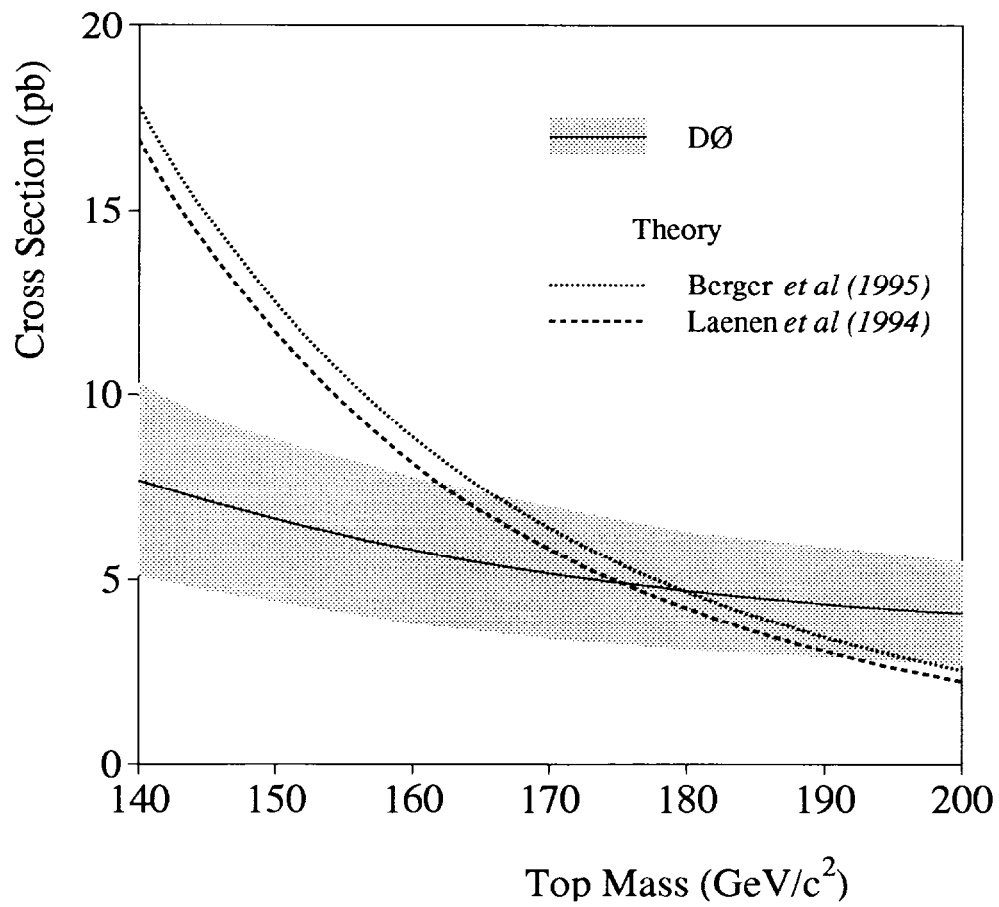


Figure 5:  $\sigma(p\bar{p} \rightarrow t\bar{t})$  vs  $m_t$ . The solid line is the DØ central value and the shaded band represents the uncertainties. The two broken lines represent the central values of theoretical predictions.

Table 5: Summary of the counting experiment in dilepton and single-lepton channels and the cross-sections for  $m_t = 180$  GeV

Channel	$\int \mathcal{L} dt$ [ $\text{pb}^{-1}$ ]	Background	Expected Signal	Data	$\sigma$ [pb]
$ee$	105.9	$0.66 \pm 0.17$	$0.92 \pm 0.11$	1	$4.59 \pm 3.14$
$\mu\mu$	86.7	$0.55 \pm 0.28$	$0.53 \pm 0.11$	1	
$e\mu$	90.5	$0.36 \pm 0.09$	$1.69 \pm 0.27$	3	$3.85 \pm 1.93$
$e + jets$ (shape)	105.9	$3.81 \pm 1.41$	$6.46 \pm 1.38$	10	
$\mu + jets$ (shape)	95.7	$5.42 \pm 2.05$	$6.40 \pm 1.51$	11	$6.82 \pm 3.21$
$e + jets$ (tag)	90.5	$1.45 \pm 0.42$	$2.43 \pm 0.42$	5	
$\mu + jets$ (tag)	95.7	$5.42 \pm 2.05$	$6.40 \pm 0.92$	6	
All	$\sim 100$	$13.4 \pm 3.0$	$21.2 \pm 3.8$	37	$4.7 \pm 1.6$

$$\sigma(p\bar{p} \rightarrow t\bar{t}) = 4.7 \pm 1.6 \text{ pb.}$$

Figure 5 shows the top pair production cross-section as a function of the mass of the top quark. Our results agree with theoretical calculations within a  $\sim 30$  GeV window centered at about 177 GeV even without taking the theoretical uncertainties into account.

## 5 Summary

Since the observation of top a year ago, there have been significant improvements in the  $D\bar{O}$  top analysis. The data set has doubled, we have much better particle-identification tools, and the event selection criteria have been re-optimized to minimize the error on the top production cross section. Preliminary results have been presented for dilepton and two orthogonal lepton + jets analyses. The details of the individual channels are summarized in Table 5. The correlation between the channels have been taken into account in the calculation of the uncertainties. Altogether, we observe 37 events in our data sample with an estimated  $13.4 \pm 3.0$  events from background processes. The resultant cross section is a function of the mass of the top quark. For  $m_t = 180$  GeV, we get  $\sigma(p\bar{p} \rightarrow t\bar{t}) = 4.7 \pm 1.6$  pb which is in excellent agreement with the theoretical prediction of  $4.9 \pm 1.0$  pb.

## Acknowledgments

We thank the staffs at Fermilab and the collaborating institutions for their contributions to the success of this work, and acknowledge support from the Department of Energy and National Science Foundation (U.S.A.), Commissariat à l'Énergie Atomique (France), Ministries for Atomic Energy and Science and

Technology Policy (Russia), CNPq (Brazil), Departments of Atomic Energy and Science and Education (India), Colciencias (Colombia), CONACyT (Mexico), Ministry of Education and KOSEF (Korea), CONICET and UBACyT (Argentina), and the A.P. Sloan Foundation.

### References

1. DØ Collaboration, S. Abachi *et al.*, Phys. Rev. Lett. **74**, 2632 (1995).
2. CDF Collaboration, F. Abe *et al.*, Phys. Rev. Lett. **74**, 2626 (1995).
3. E. Laenen, J. Smith, and W. van Neerven, Phys. Lett. **321B**, 254 (1994).
4. N. Amos, these proceedings.
5. F. Paige, S. Protopopescu, BNL Report BNL38034, 1986 (unpublished), v6.49.
6. F. Carminati *et al.*, "GEANT Users' Guide", CERN Program Library, December 1991 (unpublished).
7. T. Sjöstrand, "PYTHIA 5.6 and JETSET 7.3", CERN-TH.6488/92, May 1992 (unpublished)
8. W. T. Giele, E. Glover, D. Kosower, Nucl. Phys., **B403**, 633, (1993).
9. G. Marchesini *et al.*, Computer Physics Communications, **67**, 465 (1992).
10. F. A. Berends, H. Kuijf, B. Tausk, and W.T. Giele, Nucl. Phys. **B357**, 32 (1991).
11. S. Abachi *et al.*, Phys. Rev. D **52**, 4877 (1995).